

Photocatalytic discoloration of organic compounds on outdoor building cement panels modified by photoactive coatings

T. Yuranova^a, V. Sarria^{a,b}, W. Jardim^c, J. Rengifo^a, C. Pulgarin^a,
G. Trabesinger^d, J. Kiwi^{a,*}

^a SB ISIC-LGRC, Ecole Polytechnique Fédérale de Lausanne (EPFL), 1015 Lausanne, Switzerland

^b Department of Chemistry, Uni-Andes, Cra1 E18A-10, Bogota, Colombia

^c Chemical Institute, State University of Campinas (UNICAMP), Brazil

^d Eternit AG, CH-8867 Niederurnen, Switzerland

Received 2 November 2006; received in revised form 12 December 2006; accepted 19 December 2006

Available online 27 December 2006

Abstract

Cement based Eternit plates modified by TiO₂/SiO₂ surface layers acquired self-cleaning properties. The TiO₂/SiO₂ coating was transparent indicating that the small TiO₂ (rutile) crystals cause no significant scattering. The parameters related to the composition of the TiO₂/SiO₂ coating were investigated in relation to concentration and ratio of the components and the time and temperature necessary for the colloid networking to produce the self-cleaning effect. The repetitive discoloration of natural pigments on the TiO₂/SiO₂/Eternit plates was observed showing the stable performance of the TiO₂/SiO₂ coating. FTIR spectroscopy shows the stability of the acrylic and cellulose components on the TiO₂/SiO₂/Eternit plates after repetitive self-cleaning cycles. A self-cleaning mechanism is suggested in agreement with the experimental findings. The SiO₂ layers seem to avoid the radical attack on the acrylic topmost layers of the Eternit plates due to the TiO₂ (h⁺_{vb}) generated under solar simulated radiation. The profile and thickness of the coating was estimated by confocal microscopy. X-ray diffraction showed that the Eternit plates had a structure forming function on the TiO₂/SiO₂ layers leading to the formation of rutile from the Ti-colloids at temperatures as low as ~80 °C.
© 2007 Elsevier B.V. All rights reserved.

Keywords: Self-cleaning; Cement panels/plates; Daylight radiation; SiO₂/TiO₂ colloids

1. Introduction

The use of TiO₂ mediated photocatalysis for the abatement of pollutants, non-bio-degradable compounds and toxic residual materials in the gas, liquid and solid phase has been the subject of many recent studies and monographies [1–3].

In the past decade several attempts have been carried out at the academic [4] and industrial level [5,6] to coat cement building outdoor and indoor panels with wax and heavy paraffin's of diverse compositions. The intention was to mimic the protective effect found in *Nelumbo nucifera* (Lotus effect) by which a structured hydrophobic film protects the leaves of dirt and other damaging effects due natural elements and foreign bodies. But the hydrophobic coating applied with this purpose deteriorated with time when exposed to natural elements and

the UV-component of solar irradiation. In effect, this approach failed for three reasons: (a) the polymers used were destroyed by weathering within months or years, (b) cracks were seen to develop in the polymers after a few months and (c) the high cost of the coatings [7,8]. The corrosion of bare cement plates is due to the leaching of Ca²⁺-ion of the CaCO₃ component of these plates. This destroys the high intrinsic initial alkaline pH of these panels. This is caused by the atmospheric CO₂ and water vapor reaching the building panel and diffusing into the surface and bulk of the cement (carbonation). This situation has prompted industrial and academic laboratories to look into this problem to find a solution that is technically feasible and economically possible.

We intent to coat cement building wall panels and test the self-cleaning effect of the coating under daylight on natural pigments. The self-cleaning action consists in the destruction of organic stains on the coating layers containing TiO₂ due to light irradiation in the presence of atmospheric O₂. Our laboratory has recently gained experience in the photocatalytic coatings

* Corresponding author.

E-mail address: john.kiwi@epfl.ch (J. Kiwi).

effective in the discoloration of organic colored compounds on supports as: Nafion-membranes [9], thin film polyethylene-maleic anhydride films [10], surface modified glass mats [11], polyamide and polyester based textile [12] and cotton textiles [13]. The outstanding photo-catalytic properties of TiO_2 recommend its use in surface coating with self-cleaning properties. This idea is simple, but the application of stable and performing TiO_2 transparent layers adapted to a particular substrate is difficult.

The objective of this work is to coat SiO_2 to protect the acrylic topmost layer of the Eternit plates from the attack of highly oxidative radicals produced by TiO_2 under light irradiation. During the course of this work a large number of preliminary experiments were carried out to optimize the most suitable composition of the $\text{SiO}_2/\text{TiO}_2$ layers on the cement Eternit outdoor panels.

The self-cleaning discoloration kinetics on the $\text{TiO}_2/\text{SiO}_2/\text{Eternit}$ plates was evaluated during the photodegradation of natural pigments and tested during repeated cleaning cycles to demonstrate the stable photocatalytic nature of the coating. The most active samples of $\text{TiO}_2/\text{SiO}_2/\text{Eternit}$ plates were characterized by four different techniques: attenuated total reflection infrared spectroscopy (ATRIR), confocal microscopy, optical microscopy (OM) and X-ray diffraction (XRD).

2. Experimental

2.1. Materials

Reagents like acid and bases, dyes, tetra-ethoxysilane (TEOS), Ti-tetra-isopropoxide (TTIP) were p.a. from Fluka AG Buchs, Switzerland and used without further purification. Millipore-Q tri-distilled H_2O was used throughout this study. Ludox SM-30% ex-Dupont de Nemours was a gift of Grace GmbH, 4153, Rheinach, Switzerland. The colloid contained SiO_2 30 wt% negatively charged and equilibrated at pH 9.9 with particles having sizes of 7–8 nm and a specific surface area of $360\text{ m}^2/\text{g}$. These silica dispersions are often used to increase the resistance to friction of diverse surfaces mainly in the textile and ceramic industry. The preformed plates containing mainly cement, cellulose and binders were a gift of Eternit AG, Niederurnen 8867, Switzerland. These plates of fiber cement have the following make up: cement 80%, cellulose 4%, polyvinyl-alcohol 2%, CaCO_3 ~1% and binders. In order to avoid the leaching out of Ca^{2+} to the surface, these outdoors panels are covered with a thin acrylic film $30\text{ }\mu\text{m}$ thick.

2.2. Preparation of coated samples of $\text{TiO}_2/\text{SiO}_2/\text{Eternit}$ plates

The coating of the samples was performed in three different steps: (a) the plates were immersed in a solution of TEOS in 2-propanol water solution. The make up of this solution comprised 10 ml TEOS, 75 ml of 2-propanol with 2.5 ml HCl and 2.5 ml of water. After immersion, the plates were let dry at room temperature, (b) subsequently, the plates were immersed in the mixture of two colloids SiO_2 (Ludox, 30%) and a TTIP 5%

stock solution diluted with water four times and (c) then, the plates were dried at room temperature and heated to $80\text{ }^\circ\text{C}$ for 2 h. The temperature applied for the SiO_2 cross-linking on the plates is limited by the thermal temperature limit of the cellulose component ($80\text{ }^\circ\text{C}$) of the Eternit plates.

The TTIP stock solution used in step (b) was prepared in the following way: 5 ml TTIP were mixed with 1 ml acetic acid, 100 ml of water and 0.7 ml concentrated nitric acid. This mixture was heated to $80\text{ }^\circ\text{C}$ under steering during 30 min and further kept for 2 h under steering in the absence of heat.

2.3. Irradiation procedure during the plates self-cleaning action

The photochemical reactor consisted of 80 ml cylindrical Pyrex flasks. This reactor could accommodate the $2.5\text{ cm} \times 2.5\text{ cm}$ $\text{TiO}_2/\text{SiO}_2/\text{Eternit}$ plates. Irradiation of the samples was carried out in the cavity of a Suntest solar simulator (Hanau, Germany), air-cooled at $45\text{ }^\circ\text{C}$. The Suntest lamp emitted 5–6% of the photons within the 290 and 400 nm spectral range. The profile of the photons emitted between 400 and 800 nm followed the solar spectrum with a light intensity of 50 mW cm^{-2} corresponding to 50% of AM1 (AM1 corresponding to the light intensity of the midday equatorial solar radiation). The radiant flux was monitored by a LSI Corporation power meter of Yellow Springs, Co., USA. In a typical experiment a drop of red wine containing mainly the pigment tannin, carotene and lycopene was dispersed on the $\text{TiO}_2/\text{SiO}_2/\text{Eternit}$ plate. The discoloration was followed quantitative as a function of time at selected intervals by diverse techniques as described below in Section 3.

2.4. Monitoring the CO_2 during the stain mineralization

The CO_2 produced during irradiation was measured in a gas chromatograph (Carlo Erba, Milano) provided with a Poropak S column.

2.5. Fourier transform infrared spectroscopy

The detailed description of the applied internal reflection FTIR technique and procedure used have been previously reported [16]. The infrared reflection spectra of the catalyst samples were recorded on a Bruker IFS55 FTIR spectrometer equipped with an MCT detector and a reflection ATR attachment. A ZnSe reflection element ($47 \times 20 \times 3$) with incident angle 45° was used in these studies. These accessories were from Harrick Scientific Co. The unit of intensity was defined as $-\log(R/R_0)$, where R_0 and R are the reflectivities of the element under analysis and of the element on the $\text{TiO}_2/\text{SiO}_2/\text{Eternit}$ surface, respectively. Both sample and reference spectra were averaged over the same number of 1000 scans.

2.6. Confocal microscopy

Confocal microscopy is used increasingly for the investigation of films having thickness in the micron range since the

reflection optics makes possible a resolution and depth of focus beyond the limit of a normal optical microscope. The system consists of a camera head, a control unit and a monitor and provides a high-resolution image generation since the system can detect the signals at any point of the image (Nikon Optiphot). In a confocal microscope, the sample surface is scanned by He–Ne laser of 6 mW power and the microscope is provided with an acousto-optic modulator which deviates the laser beam as function of the modulation applied on the crystal. The only signals detected are the ones that pass through the pin-hole behind the photo-detector over the whole surface of the image. The reflected light by the sample come back and is detected to register and store the signal. Confocal microscopy uses two lenses in a way that the plane of the image due to the first lens overlaps with the plane of the second lens and allows the analysis of the $\text{TiO}_2/\text{SiO}_2/\text{Eternit}$ surfaces with a high irregular profile accounting for a detailed topography of the sample topmost layers.

2.7. Optical microscopy

The work reporting SEM of the $\text{TiO}_2/\text{SiO}_2/\text{Eternit}$ surfaces have been carried out with a Philips AM optical microscope.

2.8. X-ray diffraction measurements of TiO_2 loaded textiles

The crystallinity and phase of the TiO_2 loaded on the $\text{TiO}_2/\text{SiO}_2/\text{Eternit}$ plates was studied with a Siemens X-ray diffractometer using $\text{Cu K}\alpha$ radiation source.

3. Results and discussion

3.1. Preparation of the $\text{TiO}_2/\text{SiO}_2/\text{Eternit}$ coatings

Due to the strong oxidative activity of TiO_2 these films should not be applied directly on the acrylic topmost layer of the Eternit plates [1–3]. Silica has been often used as a binder and an inert protecting layer to anchor TiO_2 on surfaces designed to sustain long-term operational stability under light irradiation [14]. The SiO_2 as used in this study in the form of colloid or films when applied to surfaces have two functions: (a) they act as a binder for the TiO_2 particles and (b) they also acts as a barrier layer to prevent damage/corrosion on the acrylic film during the photocatalytic discoloration.

Fig. 1 shows the SiO_2 hydrophobic layer deposition on the panel surface. A long series of preliminary tests did show that two layers of SiO_2 of different sources produced the best pho-

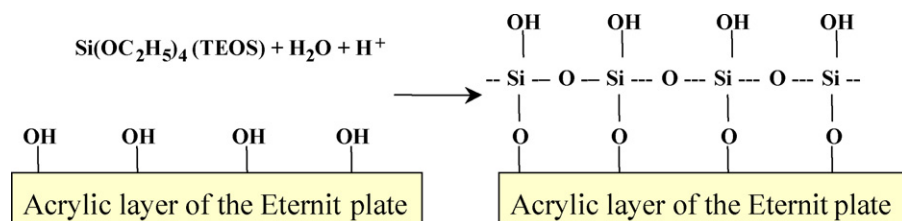


Fig. 1. Schematic of the deposition of the more hydrophobic SiO_2 TEOS based layer on the cement Eternit panels.

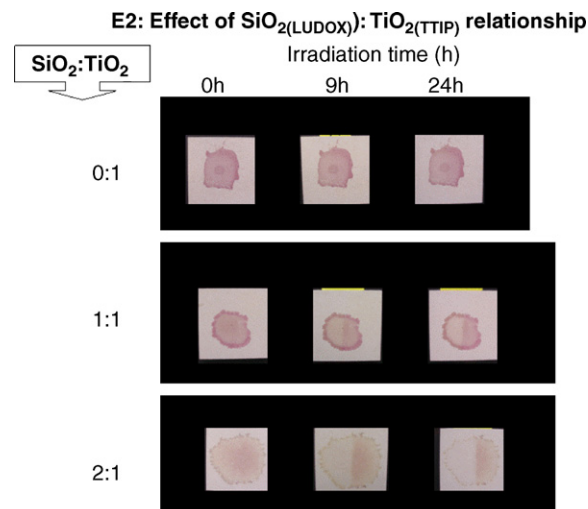


Fig. 2. Dependence of the discoloration of a red wine stain on the ratio between the SiO_2 and TiO_2 as a function of time under Suntest daylight irradiation (90 mW cm^{-2}). The times from left to right are 0, 3 and 6 h, respectively. The first row refers to the $\text{SiO}_2:\text{TiO}_2$ ratio of 0:1, and the second and third row refer to ratios of 1:1 and 2:1, respectively.

todiscoloring effects for stains on the $\text{TiO}_2/\text{SiO}_2/\text{Eternit}$ plates. This was carried out using two sources of SiO_2 , a TEOS based colloidal layer first applied on the topmost hydrophobic acrylic layer of the Eternit plates as shown below in Fig. 1, followed by an hydrophilic colloidal SiO_2 layer from an aqueous dispersion (Ludox colloid SM30). This led to the most suitable discoloration kinetics of the wine stain under light irradiation. It has been recently shown that anatase phase was formed on sol–gel $\text{SiO}_2/\text{TiO}_2$ coatings needing only water vapor or hot water treatment [15]. The formation of anatase was reported to proceed through several stages involving the hydrolysis of Si–O–Ti bonds, dissolution of the SiO_2 component, subsequent migration of the hydrolyzed TiO_2 and finally nucleation followed by growth of the TiO_2 crystals. During the synthesis of the $\text{SiO}_2/\text{TiO}_2$ colloid, the hydrolysis, dissolution and crystallization of the colloids strongly varied as a function of the temperature, solution pH concentration of the reagents selected for the process shown schematically in Fig. 1.

3.2. Self-cleaning of red wine stains on $\text{TiO}_2/\text{SiO}_2/\text{Eternit}$ plates

Fig. 2 shows the effect of the $\text{SiO}_2:\text{TiO}_2$ ratio on the self-cleaning kinetics of the red wine stain under simulated solar irradiation. The upper column shows that in the absence of

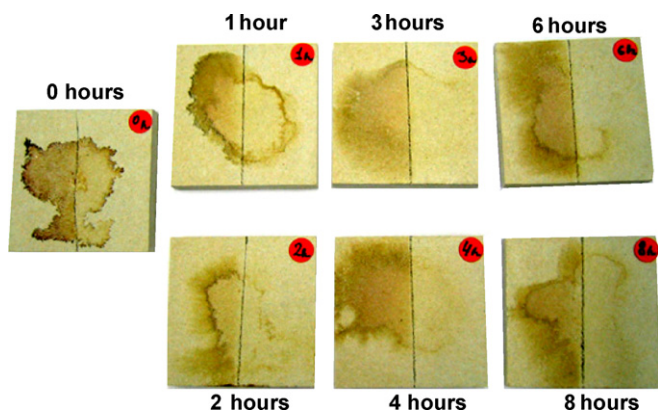


Fig. 3. Dependence of the discoloration of a red wine stain on the thermal treatment time of the $\text{TiO}_2/\text{SiO}_2$ coating on the Eternit panels at 80°C . Suntest simulator daylight irradiation intensity set at 90 mW cm^{-2} .

the SiO_2 layer, the photodiscoloration did not proceed up to 24 h irradiation. A colloidal ratio of 1:1 as shown in column 2 lead to a slower photodiscoloration than when a ratio $\text{SiO}_2:\text{TiO}_2 = 2:1$ was employed. Fig. 3 shows the photodiscoloration for $\text{TiO}_2/\text{SiO}_2/\text{Eternit}$ surfaces as a function of the heating time during preparation the coating up to 8 h. It is readily seen that after 2 h the photodiscoloration of the red wine stain was the most favorable.

Fig. 4 shows the complete photodiscoloration of the red wine stain on the $\text{TiO}_2/\text{SiO}_2/\text{Eternit}$ plates after 24 h irradiation in the cavity of the Suntest solar simulator.

3.3. Stability of the performance of $\text{TiO}_2/\text{SiO}_2/\text{Eternit}$ plates during stain photodiscoloration

Fig. 5 shows the discoloration performance of the $\text{TiO}_2/\text{SiO}_2/\text{Eternit}$ plates after one, three and six photodis-

coloration cycles. The photodiscoloration kinetics was conserved during each of the repetitive discoloration cycles showing the stable performance of the system. The reason for this favorable performance may be due to: (a) the procedure applied to deposit $\text{TiO}_2/\text{SiO}_2$ colloidal layers precluding radical attack on the acrylic topmost layers of the Eternit plate (b) the good adherence of the $\text{TiO}_2/\text{SiO}_2$ colloidal layers to the acrylic layer on the plates.

3.4. Mineralization of the red wine stain under solar simulated light

The photodiscoloration of the wine stain observed in Figs. 2–5 with concomitant CO_2 production was expected on the $\text{TiO}_2/\text{SiO}_2/\text{Eternit}$ plates under light irradiation in time proportional to the oxidative decomposition of red wine stain. This was not observed. No CO_2 could be detected in a closed vessel by GC analysis even after 24 h simulated solar irradiation. Then, adsorption of CO_2 under light was tried and was effectively observed on the $\text{TiO}_2/\text{SiO}_2/\text{Eternit}$ plates. This is due to the known carbonation of cement making up 80% of the Eternit plates under study [6–8].

3.5. Infrared spectroscopy of irradiated $\text{TiO}_2/\text{SiO}_2/\text{Eternit}$ plates

Fig. 6 shows the attenuated total reflection infrared spectroscopy for the discoloration process of the red wine stain and the necessary control experiments. Trace 10 shows the initial acrylic peak if the topmost layer of the Eternit plates with the characteristics bands of the acrylic group at $\sim 2900\text{ cm}^{-1}$, of the carbonyl ester at 1740 cm^{-1} and of the carboxyl group at 1430 cm^{-1} [16]. The strong band at $\sim 1000\text{ cm}^{-1}$ corresponds

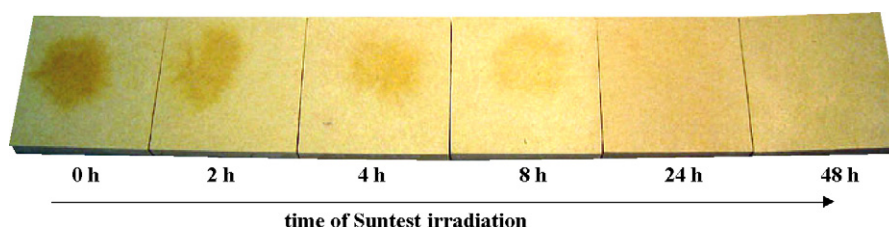


Fig. 4. Red wine stains discoloration on $\text{TiO}_2/\text{SiO}_2/\text{Eternit}$ plates as a function of irradiation time. The Eternit panels have been coated by the procedure described in Section 2. Suntest simulator (90 mW cm^{-2}).

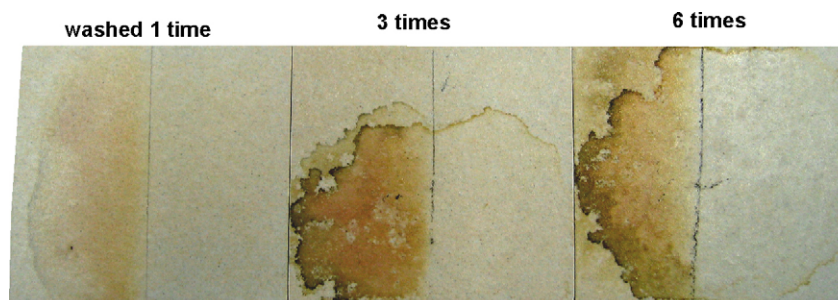


Fig. 5. Discoloration of the red wine stain on $\text{TiO}_2/\text{SiO}_2/\text{Eternit}$ plates as a function of repetitive addition of these stains on the plates. Other experimental details as reported for Fig. 4.

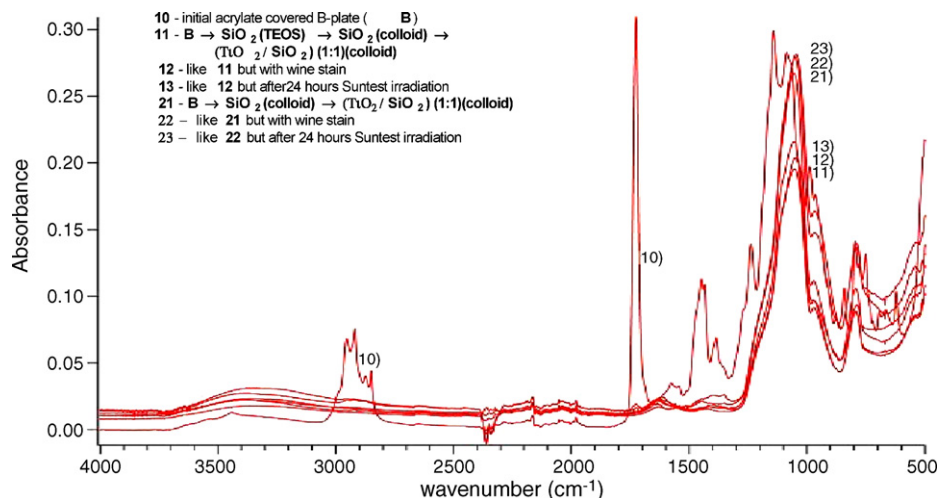


Fig. 6. Infrared spectroscopy of $\text{TiO}_2/\text{SiO}_2/\text{Eternit}$ plates without and with addition of red wine stain before and after 24 h Suntest irradiation (90 mW cm^{-2}). For other experimental details see text.

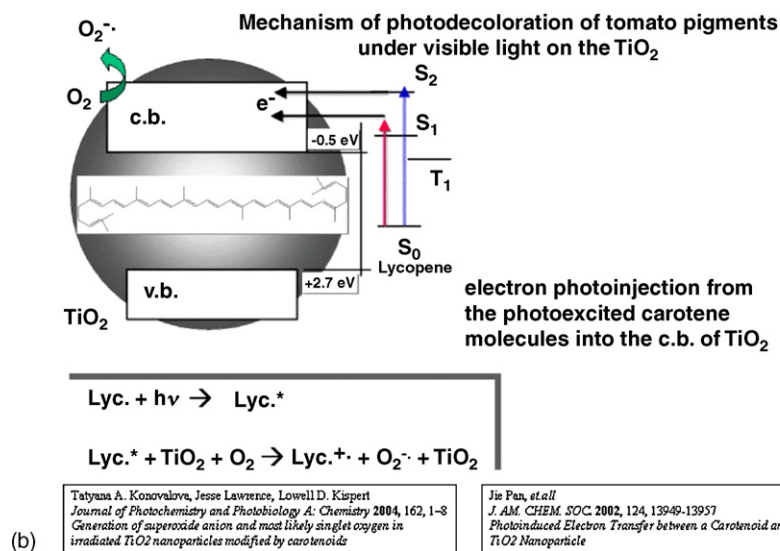
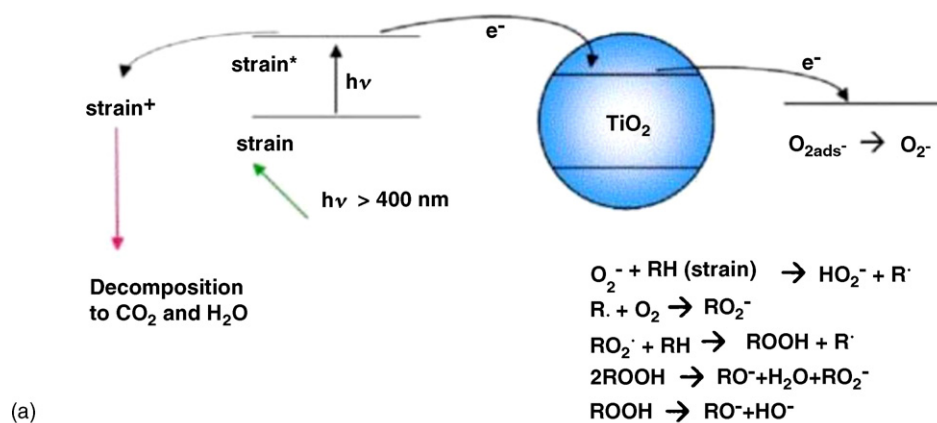


Fig. 7. (a) Scheme for the generation of highly oxidative species on the surface of TiO_2 under daylight irradiation (90 mW cm^{-2}). (b) Scheme for the photodiscoloration mechanism of the red wine stain under daylight irradiation.

to the polysaccharide groups of the cellulose component of the Eternit cement plates. The acrylic group is the acyl derived from the acrylic acid [17]. Trace 11 refers to the $\text{TiO}_2/\text{SiO}_2/\text{Eternit}$ plates without the addition of red wine. In this case the stretching vibration of the Si–O–Si at $\sim 800\text{ cm}^{-1}$ is readily seen [18]. Trace 12 refers to the IR-band of the stain of wine on the non-coated with $\text{TiO}_2/\text{SiO}_2$ Eternit plate. In this case the stretching vibration of the Si–O–Si group at $\sim 800\text{ cm}^{-1}$ is readily seen. Trace 13 corresponds to the $\text{TiO}_2/\text{SiO}_2/\text{Eternit}$ plates stained with red wine after 24 h irradiation showing a peak with reduced amplitude around $\sim 1000\text{ cm}^{-1}$ [19]. A second set of experiments taking another zone of the $\text{TiO}_2/\text{SiO}_2/\text{Eternit}$ plates is shown in Fig. 7 by the peaks 21, 22 and 23 having the same characteristics of the runs 11, 12, and 13, respectively. This is necessary due to the heterogeneity of the surface of the $\text{TiO}_2/\text{SiO}_2/\text{Eternit}$ plates and is reflected in a change in the amplitude of the peaks observed between these two series of IR runs. The IR runs have been set at a relative optical absorption of 0.20. In this way, the interference of CO_2 and water vapor will not have a significant effect on the IR-measurements. After the irradiation of the red wine stained $\text{TiO}_2/\text{SiO}_2/\text{Eternit}$ plates, the surface was scratched to see whether (a) the acrylic band at 2900 cm^{-1} or (b)

the polysaccharide band at $\sim 1000\text{ cm}^{-1}$ were present still after the photodiscoloration process. This confirmed the preservation and stability of the Eternit plates after the photocatalysis.

3.6. Suggested photodiscoloration mechanism of wine stains

Fig. 7a shows the accepted mechanism for the decomposition of dyes during the last few years allowing the generation of highly oxidative radicals and H_2O_2 on the TiO_2 surface when light with $\lambda > 400\text{ nm}$ is used to photo-activate colored compounds [2,12,14]. The electron injected into the TiO_2 conduction band starts the oxidative radical-chain leading in later steps to stain discoloration. The decomposition of the stain goes through an unstable intermediate cation noted as (stain^+).

Fig. 7b suggest the scheme for the discoloration of the pigments carotene or lycopene due to the generation of OH^\bullet , HO_2^\bullet and H_2O_2 on the TiO_2 surface. The carotene and lycopene are pigments found in plants and fruits and red wine. These pigments give a deep red color to tomatoes and other vegetables. The scheme shown in Fig. 7b based on the work by the two authors noted therein, suggests that carotene and lycopene sensitize a

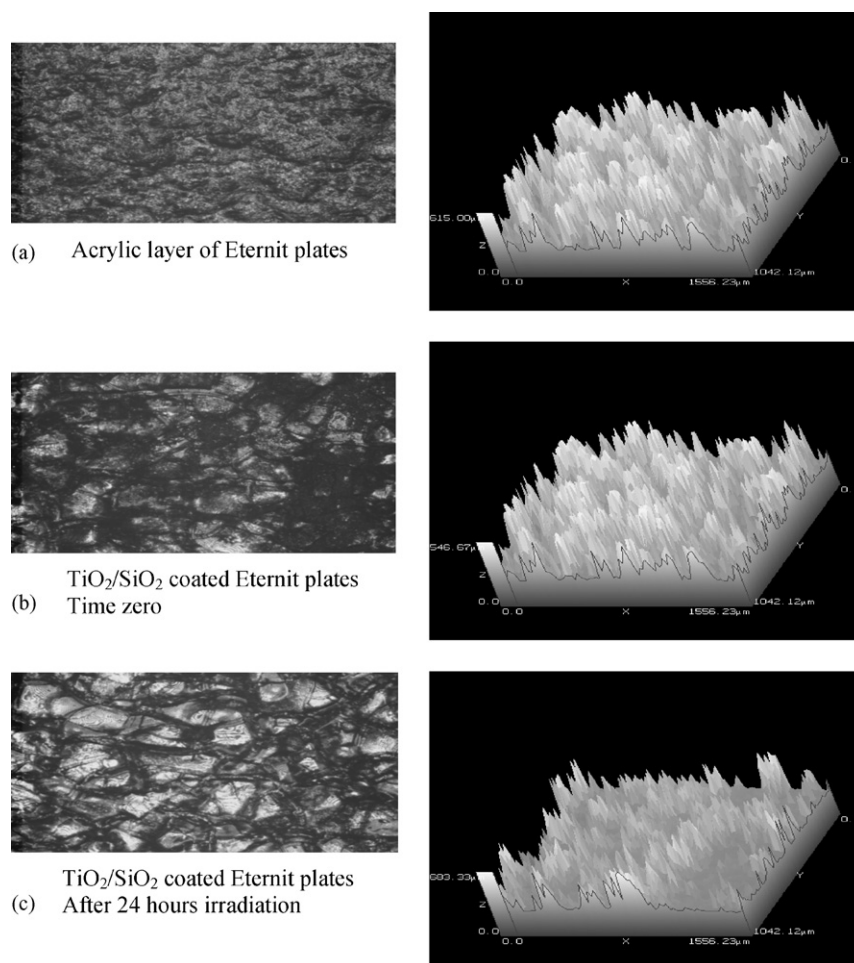


Fig. 8. Confocal microscopy of: (a) non loaded Eternit plates, (b) $\text{TiO}_2/\text{SiO}_2/\text{Eternit}$ plates before irradiation and (c) $\text{TiO}_2/\text{SiO}_2/\text{Eternit}$ plates after 24 h irradiation with a Suntest simulator (90 mW cm^{-2}).

discoloration process involving the formation of intermediate cation radicals decomposing during the discoloration process. The electron photo-injection from the excited tannin molecule into the conduction band of TiO_2 has also been reported as shown in the two reference inserted in the scheme in Fig. 8b. This pigments are also found in red wine, berries and a variety of other natural products.

3.7. Confocal microscopy studies of $\text{TiO}_2/\text{SiO}_2/\text{Eternit}$ surfaces

Fig. 8a–c show the results obtained by confocal microscopy of the non-coated and coated Eternit plate surfaces under different conditions. The left hand side column in Fig. 8 shows by the image in Fig. 8a, the acrylic layer at time zero. Fig. 8b shows that by adding the red wine on the TiO_2 particles become partially covered by the wine stain. After 24 h light irradiation the $\text{TiO}_2/\text{SiO}_2$ coating has destroyed the red wine stain as shown in Fig. 8c. This allows the TiO_2 particles to be much more visible on the cement plate surface.

The confocal microscopy has been selected to analyze the irregular profile of the surfaces showing valleys and peaks with dimensions in the micron range (Fig. 8) since this is not possible with atomic force microscopy (AFM). Fig. 8a shows a maximum height of $615\text{ }\mu\text{m}$ for the topmost acrylic layers adhering on the Eternit plates. The clearer areas in Fig. 8 refer to the density of the peak heights and the darker grey areas show the valleys in the coating layers. In Fig. 8b, it is observed that the maximum height attained by the peaks was $546.7\text{ }\mu\text{m}$ at time zero (before irradiation). This indicates that the $\text{TiO}_2/\text{SiO}_2$ coating smooth out the acrylic peaks on the topmost layer of the Eternit panels. The retention of wine on the $\text{TiO}_2/\text{SiO}_2$ on the acrylic layer depends on the surface rugosity (R_q) of the coating. Fig. 8c shows a change in the maximum peak height ($683.3\text{ }\mu\text{m}$) and in the distribution peaks and valleys compared with Fig. 8b after 24 h irradiation. The difference between the peaks and the valleys increases with respect to the values reported in Fig. 8b. This points out to the modification of the $\text{TiO}_2/\text{SiO}_2$ layers in contact with the wine stain during the photocatalysis. In Fig. 8a–c, the thickness of the acrylic layer could not be quantified with accuracy, but was estimated in the range of $\sim 300\text{ }\mu\text{m}$. The real distance from the valleys to the peaks in Fig. 8 could not be estimated accurately since we could not separate the $\text{TiO}_2/\text{SiO}_2$ coating from the underlying topmost Eternit acrylic layer. Due to this reason it was not possible to estimate the mean square roughness or rugosity from the results presented in Fig. 8. Ellipsometry has been used to measure the thickness of flat SiO_2 layers on different supports [2,20].

3.8. Optical microscopy of the $\text{TiO}_2/\text{SiO}_2/\text{Eternit}$ plates

Fig. 9 shows the optical microscopy observations for the $\text{TiO}_2/\text{SiO}_2/\text{Eternit}$ plates before undergoing any photodiscoloration process. As seen from Fig. 9, the size of the SiO_2 and TiO_2 particles were small enough to produce transparent films. The non-continuous $\text{TiO}_2/\text{SiO}_2$ layer did not change after



Fig. 9. Optical of $\text{TiO}_2/\text{SiO}_2/\text{Eternit}$ plates at time zero.

24 h irradiation. The same experimental conditions were used as employed in Figs. 2–6 of this study. The $\text{TiO}_2/\text{SiO}_2$ layer shown in Fig. 9 was observed to be stable when used in repetitive photodiscoloration cycles. The irregular structure of the acrylic film on the topmost Eternit plates originate the cracks seen in the $\text{TiO}_2/\text{SiO}_2$ layers adhering to the irregular substrate in Fig. 9. The close adherence of the $\text{TiO}_2/\text{SiO}_2$ layers to the irregular acrylic film obliges the $\text{TiO}_2/\text{SiO}_2$ film to adapt to the underlying shape with diverse geometries. Work is under way to eliminate the formation cracks in the $\text{TiO}_2/\text{SiO}_2$ layers by using a photoactive thinner coatings. As seen from Fig. 9, the size of the SiO_2 and TiO_2 particles were small enough to produce transparent films.

3.9. X-ray diffraction measurements

The crystalline phase of the TiO_2 existing on the $\text{TiO}_2/\text{SiO}_2/\text{Eternit}$ plates was investigated by XRD and the results are shown in Fig. 10. Fig. 10 shows the dotted N5 XRD spectra that the Eternit plates by themselves do not present TiO_2 related peaks. The spectra N6 correspond to the $\text{TiO}_2/\text{SiO}_2/\text{Eternit}$ plates showing the peaks of rutile at $\theta = 27.8^\circ$, 36.7° and 41.8° . Since only amorphous TiO_2 is expected at temperatures of $\sim 80^\circ\text{C}$ used during the preparation of the $\text{TiO}_2/\text{SiO}_2$ coatings, the Eternit acrylic covered plate must have a structure forming function on the amorphous TiO_2 -colloids. Recently, the formation of rutile at temperatures at $\sim 100^\circ\text{C}$ on cotton textiles [21] and wool polyamide has been reported starting from TiO_2 colloids [12]. The formation of rutile in $\text{TiO}_2/\text{SiO}_2$ coatings has been suggested along the lines reported for the formation of anatase in $\text{TiO}_2/\text{SiO}_2$ coatings [22,23]. The rutile formation would be then proceed in three steps: (a) the hydrolysis of $\text{Si}-\text{O}-\text{Ti}$ bonds, (b) the migration of the titania species in the coating from the inside out and (c) the nucleation and growth of the rutile crystals at the surface of the coating [22,23]. The rutile form of TiO_2 is less photoactive than the anatase form and should therefore be less aggressive towards the acrylic layer of the Eternit plates under light irradiation.

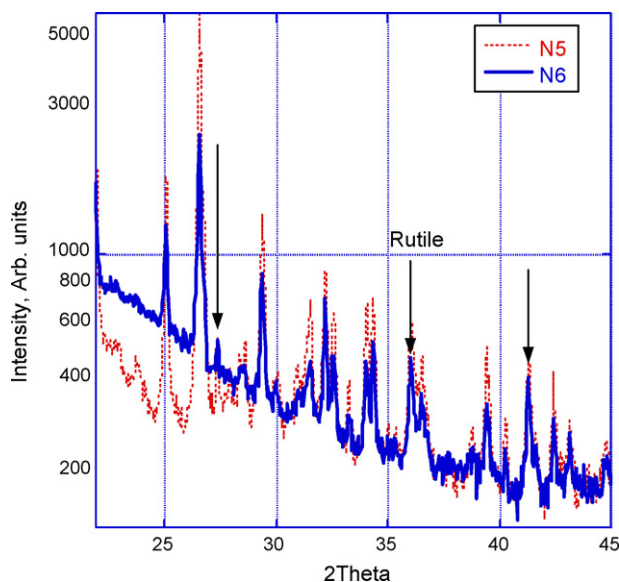


Fig. 10. X-ray diffractogram of Eternit plates (N5) and $\text{TiO}_2/\text{SiO}_2$ /Eternit plates (N6) showing the formation of the rutile phase at 80°C on the $\text{TiO}_2/\text{SiO}_2$ /Eternit plates.

This, in turn is beneficial since it would induce less chalking in the $\text{TiO}_2/\text{SiO}_2$ layers [23].

4. Conclusions

This work reports the synthesis, testing and evaluation of composite sol–gel coating layers photoactive in the discoloration of natural pigments. This study gives information on: (a) a film of $\text{TiO}_2/\text{SiO}_2$ effective in abating natural pigments prepared by sol–gel processing within the temperature limit of the Eternit panels under simulated solar irradiation, (b) the evaluation of the $\text{TiO}_2/\text{SiO}_2$ photodiscoloring activity under light irradiation, (c) the stability of the $\text{TiO}_2/\text{SiO}_2$ coating during the repetitive photodiscoloration of wine stains (used as probes) on the cement plates and (d) the properties and the structure of the $\text{TiO}_2/\text{SiO}_2$ colloidal layers deposited on the cement panels by several physical–chemical techniques. Due to the low temperature needed for the application of the $\text{TiO}_2/\text{SiO}_2$ layers on the substrate, the potential use of this procedure on low heat resistance materials (plastics) and polymer films seems warranted.

Acknowledgments

We thank the COST Action 540 PHONASUM “Photocatalytic technologies and novel nano-surface materials, critical issues”, Eternit AG, 8867, Niederurnen, Switzerland and SATW Transfer College 2004, Zurich, Switzerland for their financial support.

The help of E. Herrera de Uni-Andes, Colombia is appreciated with the microscopy work.

References

- [1] A. Fujishima, T. Rao, D. Tryk, *J. Photochem. Photobiol. C* 1 (2000) 1–21.
- [2] J. Winkler, *Titanium Dioxide*, Vincentz Network, Hanover, 2003.
- [3] M. Kaneko, I. Okura, *Photocatalysis Science and Technology*, Kodansha-Springer, Tokyo, 2002 (and references therein).
- [4] A. Mills, S.-K. Lee, *J. Photochem. Photobiol. A* 152 (2002) 233–247.
- [5] www.lion.co.jp.
- [6] www.toto.co.jp/en/index.htm.
- [7] Eternit AG, Niederurnen, Switzerland, private communication, 2005.
- [8] www.pilkington.com/pilkington/international+products/activ/default.htm.
- [9] J. Fernandez, J. Bandara, A. Lopez, Ph. Buffat, J. Kiwi, *Langmuir* 15 (1999) 185–192.
- [10] M. Dhananjeyan, J. Kiwi, Thampi, *Chem. Commun.* (2000) 1443–1444.
- [11] M. Dhananjeyan, J. Kiwi, P. Albers, O. Enea, *Helv. Chim. Acta* 84 (2001) 3433–3445.
- [12] A. Bozzi, T. Yuranova, J. Kiwi, *J. Photochem. Photobiol. A* 172 (2005) 27–34.
- [13] A. Bozzi, T. Yuranova, I. Guasaquillo, D. Laub, J. Kiwi, *J. Photochem. Photobiol. A* 174 (2005) 156–164.
- [14] A. Mills, *J. Photochem. Photobiol. A* 106 (1997) 1–35.
- [15] A. Matsuda, H. Morimoto, T. Kagure, M. Tatsumisago, T. Minami, *J. Am. Ceram. Soc.* 83 (2000) 229–234.
- [16] H.-P. Boehm, H. Knözinger, *Nature and estimation of functional groups in catalysis*, in: R. Anderson, M. Boudart (Eds.), *Science and Technology*, vol. 4, Springer-Verlag, Berlin, 1983, pp. 40–189.
- [17] <http://en.wikipedia.org/wiki/Acrylic-group>.
- [18] T. Konovalola, J. Lawrence, L. Kispert, *J. Photochem. Photobiol. A* 162 (2004) 1–8.
- [19] J. Pan, G. Genko, Y. Xu, T. Pasher, L. Sun, W. Sunstrom, T. Polivka, *J. Am. Chem. Soc.* 124 (2002) 13949–13957.
- [20] H. Honda, H. Ishizaki, R. Soma, K. Hashimoto, A. Fujishima, *J. Illum. Eng. Soc.* 42 (1988) 42–49 (and references therein).
- [21] W. Daoud, J. Xin, *J. Am. Ceram. Soc.* 87 (2004) 953–955.
- [22] Y. Kotani, A. Matsuda, T. Kogure, M. Tatsumisago, T. Minami, *Chem. Mater.* 13 (2001) 2144–2149.
- [23] H. Volz, G. Kaempf, H. Fitzky, A. Klaeren, in: P. Pappas, F. Winslow (Eds.), *ACS Symposium Series No. 151. Photodegradation and Photostabilization of Coatings*, 1981, pp. 164–182.